



Liver cancer rapid-testing POC low-cost diagnostic unit using novel dual-gate source-extended TFET based biosensor

Anirban Kolay, Amitesh Kumar^{*}

Nextgen Adaptive Systems Group, Department of Electrical Engineering, National Institute of Technology Patna, Bihar, India

ARTICLE INFO

Keywords:

Liver cancer
Rapid-Testing Diagnosis
FET
Dual-Gate TFET
Biosensors

ABSTRACT

This work discusses a rapid-testing, low-cost detection technique for Hepatocellular carcinoma (HCC) by investigating the performance of a Source Extended (SE) Tunnel Field Effect Transistor (TFET) with a Single Gate (SG) and Dual Gate (DG) configuration where the cavities are formed by etching the oxide layer beneath the gate for the immobilisation of liver samples obtained by needle biopsy. The dielectric characteristics of malignant and non-malignant liver cell lines differ at high frequencies between 100 MHz and 5 GHz. The etched nanocavities' dielectric constant changes when the sample, which were previously filled with air, are immobilised there. The shift in device drain current and performance at 900 MHz has been attributed to the specimen's change in dielectric constant. The proposed device's ON-OFF state current ratio and the difference in drain current have been used as the basis for the detection, as the purpose of the device is to differentiate the cancerous and healthy liver cell lines. The SG configuration has been analysed by modulating the adhesive layer in the cavity. A comparison has been carried out between SG and DG structures. Various parameters of the DG device, like the gate metal, channel material, and the cavities' length, have been modified to observe the performance. The investigation also included a study that took into account the varying ratios of malignant and non-cancerous samples in a certain specimen. The proposed technique of detection has been contrasted with the other documented work. To determine whether the sample of liver cell lines is malignant or not, the proposed approach can be used as a point-of-care (POC) diagnosis.

1. Introduction

To lower down cancer mortality, early diagnosis of whether or not a cell is malignant is critical [1]. Cancer causes uncontrollable cell division in the body, resulting in the destruction of other tissues. According to a World Health Organization (WHO) study, in the year 2020, over 10 million deaths occurred worldwide, nearly one in every six deaths due to cancer [2]. Cancer has been anticipated to double in the next two decades, putting a strain on human and financial resources worldwide [3]. According to WHO, liver cancer is one of the most common types of cancer in 2020, accounting for around 4.7% of all new cancer cases and 8.3% of all cancer deaths [4]. 75% to 90% of all instances of liver cancer are Hepatocellular carcinoma (HCC), which has a greater impact on cancer-related fatalities [5–7]. Cirrhosis of the liver due to hepatitis B virus (HBV) and or hepatitis C virus (HCV) viral infections, primary biliary cirrhosis, excessive alcohol consumption, Wilson's disease, and environmental exposure to aflatoxins are all risks for the development of HCC [8,9]. Ultrasound, computed tomography (CT), serum

alpha-fetoprotein (AFP) test, magnetic resonance imaging (MRI), angiography, and biopsy are some of the screening tools available for the identification of liver cancer. The most often used procedures for HCC screening are the AFP test and liver ultrasound, but the AFP test has a sensitivity of 25% to 65%, and ultrasound has a sensitivity of 60% [10]. A further important note is that tiny HCCs have ultrasound, CT scan, and MRI features comparable to non-malignant hyperplastic nodules [11,12]. As a result, screening for a disease with a large impact using these methods is not unusual. On the other hand, a biopsy is a time-consuming process in which the sample must be sent to a laboratory for evaluation, which can contain human error. Electrochemical, aptamer-based microcantilevers, carbon nanotube (CNT) and optical sensors have also been reported for the detection of liver cancer. The optical sensor detects liver cancer by sensing the HCC biomarkers AFP and alpha-1-antitrypsin (A1AT) using Surface-enhanced Raman scattering (SERS) [13]. The liver cancer cell interacted with the aptamer in the aptamer-based microcantilever sensor, causing a change in surface stress and causing the microcantilever to bend in a direction and sense to occur

^{*} Corresponding author.

E-mail address: amitesh.ee@nitp.ac.in (A. Kumar).

<https://doi.org/10.1016/j.sna.2024.115131>

Received 20 October 2023; Received in revised form 22 January 2024; Accepted 3 February 2024

Available online 7 February 2024

0924-4247/© 2024 Elsevier B.V. All rights reserved.

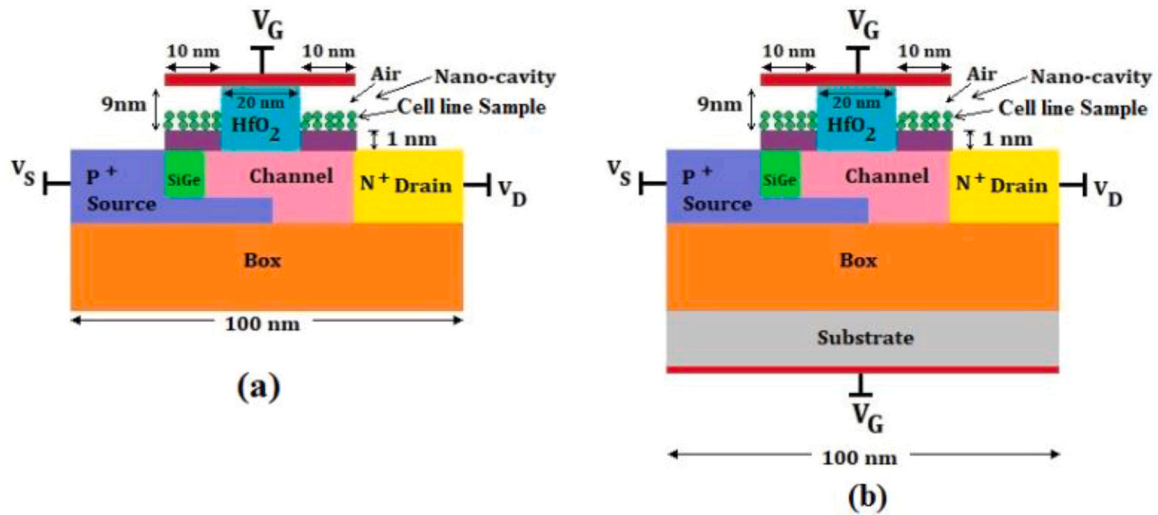


Fig. 1. Schematic diagram of the Source extended device with (a) Single gate (SG) and (b) Dual gate (DG) structure.

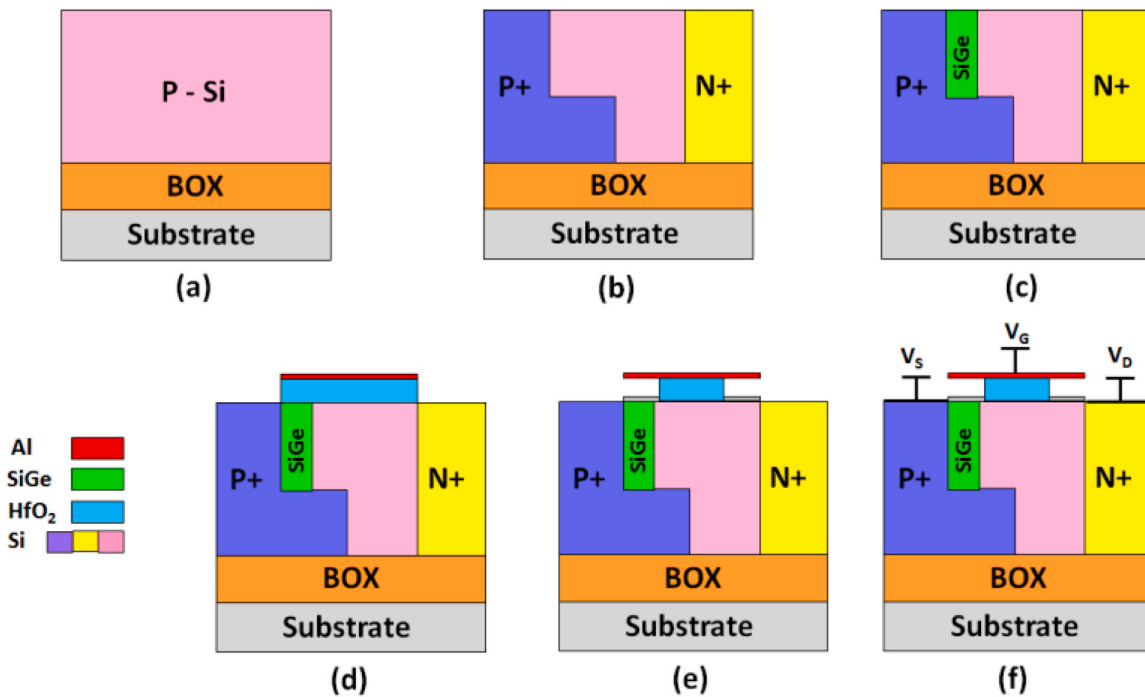


Fig. 2. Fabrication flow diagram of SESGFET Biosensor (a) Development of P-type Silicon material, (b) Deposition of P + source and N + drain, (c) Formation of SiGe layer, (d) Deposition of HfO₂ oxide layer, (e) Nano-cavity Formation, (f) Terminal employment after metallisation.

[14]. A few studies report on the electrochemical detection of malignant tissues, where the target cell is recognised by sensing the over-expressed tumour producers present on the cancer cell’s surface [15,16]. The use of carbon nanotubes (CNTs) to identify certain malignant cells has been documented in the literature [17,18]. In most of the above-reported literature, the cancerous liver cells has been detected either by detecting the HCC biomarkers or by tumor producer but in the proposed work, the liver cancer cell line sample has been considered for identification. Point-of-care (POC) detection is now essential in lowering the death rate in cancer. In the modern era, low-cost, point-of-care technologies will have a significant impact on the healthcare business and have the potential to revolutionise world health.

The field effect transistor (FET)-based biosensor is now being utilised to detect a variety of biomolecule. Bergveld was the first to develop an ion-sensitive FET-based bio-sensor in 1970 [19]. Several ion sensors

have been documented in the literature, with the performance being improved with charged biomolecules [20,21]. Various works have been published in the literature in recent times to improve the sensitivity of neutral biomolecule detection through dielectric modification of biomolecules [22–24]. Several tunnel field effect transistor (TFET) structures have been designed for bio-sensing applications to enhance sensitivity [25–27]. Several biomarkers, such as DNA, antibodies, and different proteins, have been intended for determining the presence of various cancer cells. A study on FET sensor arrays has been reported to detect bladder cancer biomarkers such as NMP22 and cytokeratin 8 (CK8) [28]. A Molybdenum disulfide (MoS₂) FET-based biosensor has been proposed, which is able to detect prostate cancer at an early stage by sensing the prostate-specific antigen (PSA) in urine samples [29]. Rajesh et al. reported that antibody-functionalised platinum nanoparticles provided graphene FET for the identification of the breast

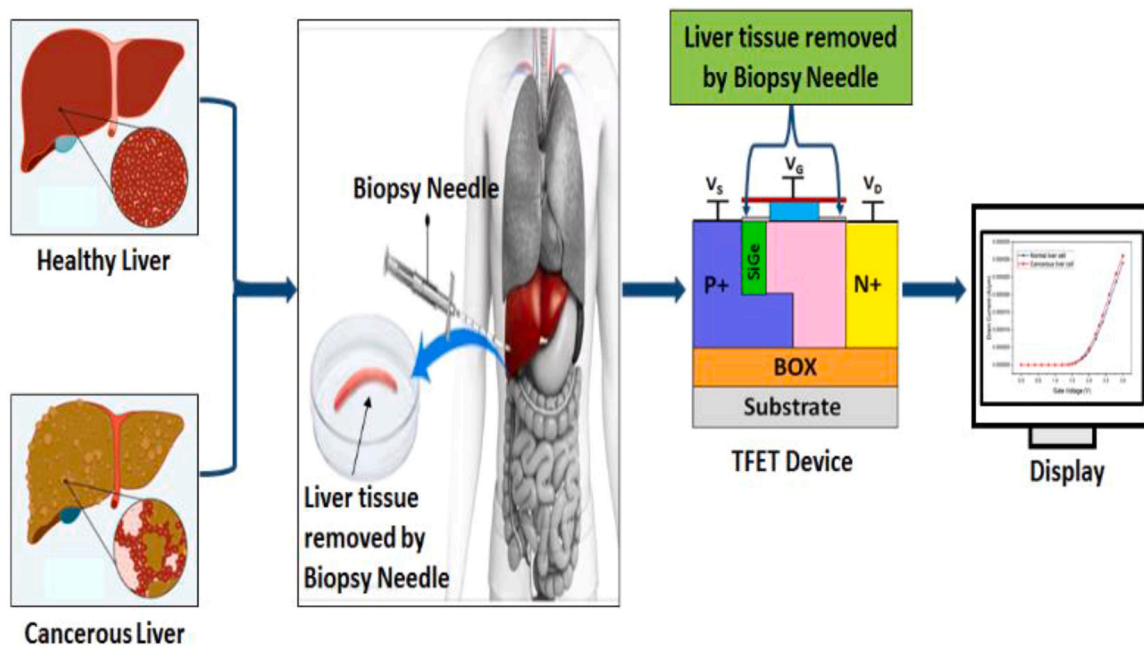


Fig. 3. Detailed representation of stages involved in Liver cancer cell lines detection, healthy or cancerous liver cell line obtained by needle biopsy samples which can be detected by proposed TFET device because of the variations in the electrical properties of the cell lines.

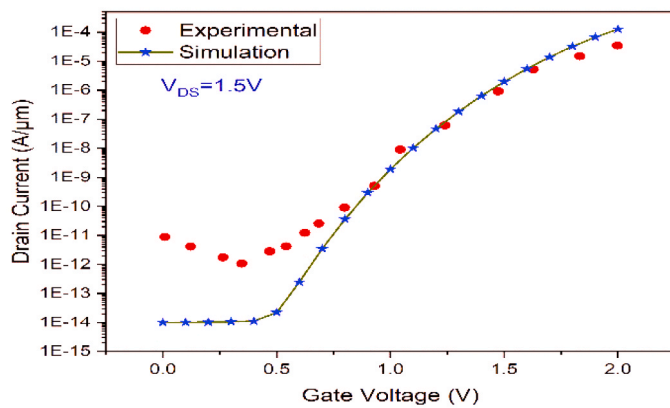


Fig. 4. Transfer Characteristics of SESGTFET model and experimental data [41] available in the literature.

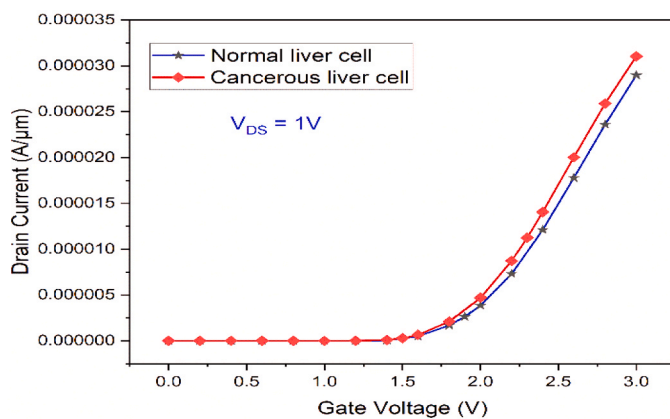


Fig. 5. Transfer Characteristics (in linear current scale) of SESGTFET device with both side cavities filled with a cancerous and non-cancerous liver sample having SiO₂ as an adhesive layer in cavities.

cancer biomarker HER3 to detect the hazard of breast cancer [30]. A DNA-FET biosensor-based microfluidic system has been proposed in the literature to detect breast cancer by identifying breast cancer biomarkers [31]. Gaojian et al. demonstrated a FET biosensor that allows the detection of neuron-specific enolase (NSE), and cytokeratin 19 fragments (CYFRA 21-1), which are the tumor markers for lung cancer [32]. Most of the reported work related to various cancer detection is based on the detection of the biomarker whereas in the proposed work, the liver cell lines have been taken into account. At microwave frequencies, certain malignant tissues exhibit some unique dielectric properties that drew the attention of researchers. Peyman *et al.* noticed a change in dielectric constants as a result of diverse clinical conditions in the human liver, with the frequency ranging from 100 MHz to 5 GHz [33]. According to the cited research, a liver tumor has a greater dielectric constant than a healthy liver tissue due to malignant liver tissue's higher sodium and water content [33]. Joines et al. demonstrated how the dielectric characteristics of several normal and malignant tissues alter when the target specimen is subjected to dielectric spectroscopy at frequencies ranging from 100 to 900 MHz [34]. As the shift in dielectric characteristics is greater at 900 MHz, it has been considered for future research. The needle biopsy described by Nuciforo *et al.* can be used to collect the liver cell line sample for the investigation [35]. Following sample extraction, the sample can be immobilised into the cavities of the proposed device for identification. Due to the insertion of the liver cell line sample in the cavities of the proposed device, the electrical characteristics of the device change, resulting in a change in the device's current, which has been considered a sensing technique. Since the change in electrical characteristics has been treated as the sensing technology in this approach, it can be used as a POC detection tool. The suggested work has been carried out using the Silvaco Atlas TCAD [36] simulator. The performance of the proposed SG device was evaluated by altering the adhesive layer in the cavity region. Various studies have been carried out for DG structure based on gate material modification, channel material modulation, cavity dimensions, and specimens with different proportions of cancer cell lines. Sections 2 and 3 of this work cover the device architecture and the sensitivity analysis with respect to the device's various controlling parameters, respectively. Section 4 compares various available approaches in the literature to the

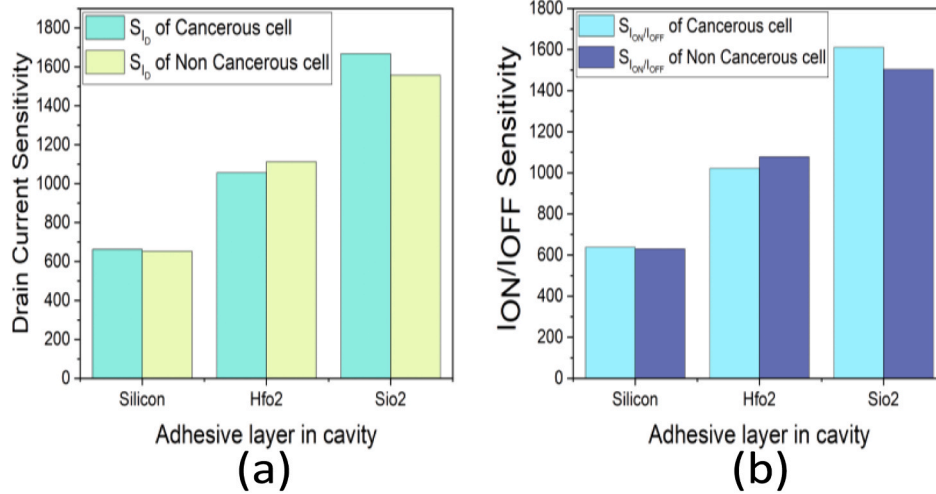


Fig. 6. (a) Drain current sensitivity, (b) I_{ON}/I_{OFF} sensitivity of SESGFET device with various materials beneath biomolecule in a cavity filled with cancerous and healthy liver cell lines.

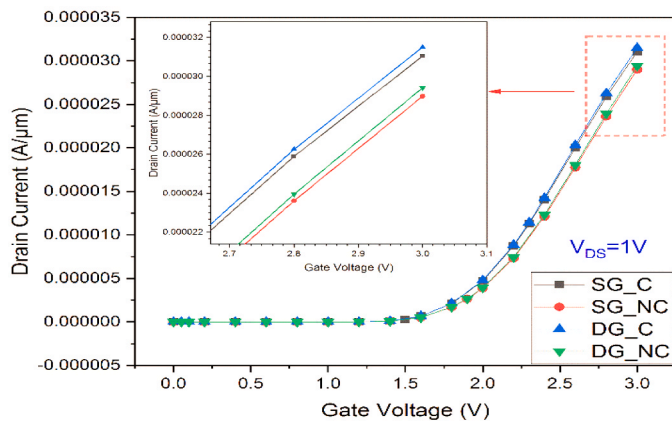


Fig. 7. $I_D - V_G$ Characteristics of silicon channel SESGFET and SEDGFET device having a gate work function of 4.2 eV.

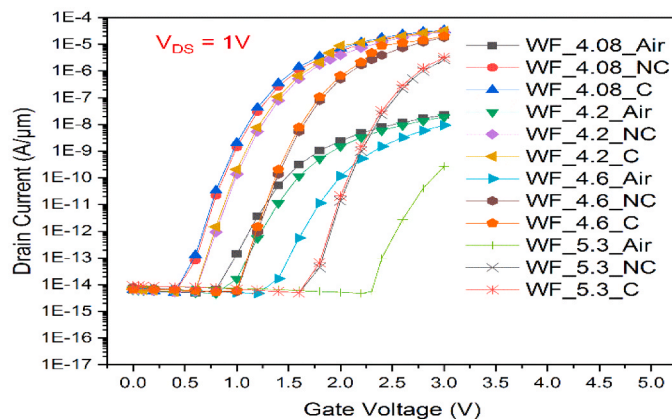


Fig. 8. $I_D - V_G$ Characteristics of silicon channel SEDGFET device for different gate work function with different cavity filling.

proposed method for detection.

2. Device architecture and design

The structure of 2D source extended single gate (SESGFET) and dual gate TFET (SEDGFET) is shown in Fig. 1(a) and Fig. 1(b) respectively. Fig. 2 shows the fabrication process of SESGFET, which includes masking and lithography followed by source and drain deposition. The area close to the source has been trenched away to make room for the SiGe layer's deposition. A 40 nm-long HfO₂ or Al gate frame can be created using the dry etching and LPCVD techniques, respectively. The nano-cavity is created afterwards by trenching 10 nm of HfO₂ away from the source and drain sides. The biomolecules are immobilised by trenching the dielectric material, which creates nano-cavities and bare silicon of 1 nm thickness in the air. A FET structure which has been used for biomolecule detection, and the cavity is in the range of 10 nm [23].

The cavities are formed near the interaction of the gate-source and gate-drain region, having a length and depth of 10 nm and 9 nm. The source, channel, and drain are made of silicon on a 20 nm thick SiO₂ layer termed as BOX. In SEDGFET the back gate has been considered below the substrate underneath the BOX. The doping concentration for highly doped p-type source and n-type drain are $1 \times 10^{20} \text{ cm}^{-3}$ and $1 \times 10^{18} \text{ cm}^{-3}$ respectively, whereas the channel concentration has been taken as $1 \times 10^{16} \text{ cm}^{-3}$. The SiGe layer has been incorporated in both devices to shorten the effective tunneling path, which results in a noticeable increase in band-to-band tunneling [37]. An increase in the mole fraction of the SiGe layer consequences a decrease in the energy band gap [38]. In dual gate structures, the gate metal and channel material have been varied, and a study has been made.

The process flow diagram has been represented in Fig. 3 where the various steps of detection procedure has been described. The liver cell line with or without cancerous cell are detected from liver samples obtained by the needle biopsy. For improved liver sample binding and a cavity region for sample immobilisation, a SiO₂ layer with a thickness of 1 nm is present. It has been presumed that the specimen must be implanted in the cavities and depending on the nature of the sample, there are differences in drain current on the basis of which the sensing has been done.

This work and analysis have been carried out on the Silvaco TCAD simulator. Due to the high doping concentration, the Doping Dependent Mobility model and the Fermi-Dirac Statistic Transport model have been considered in the analysis. For the accomplishment of the tunneling, the Band Gap Narrowing (BGN) and Non-Local Band-to-Band Tunneling (BTBT) models have been applied. The Shockley-Read-Hall (SRH) model

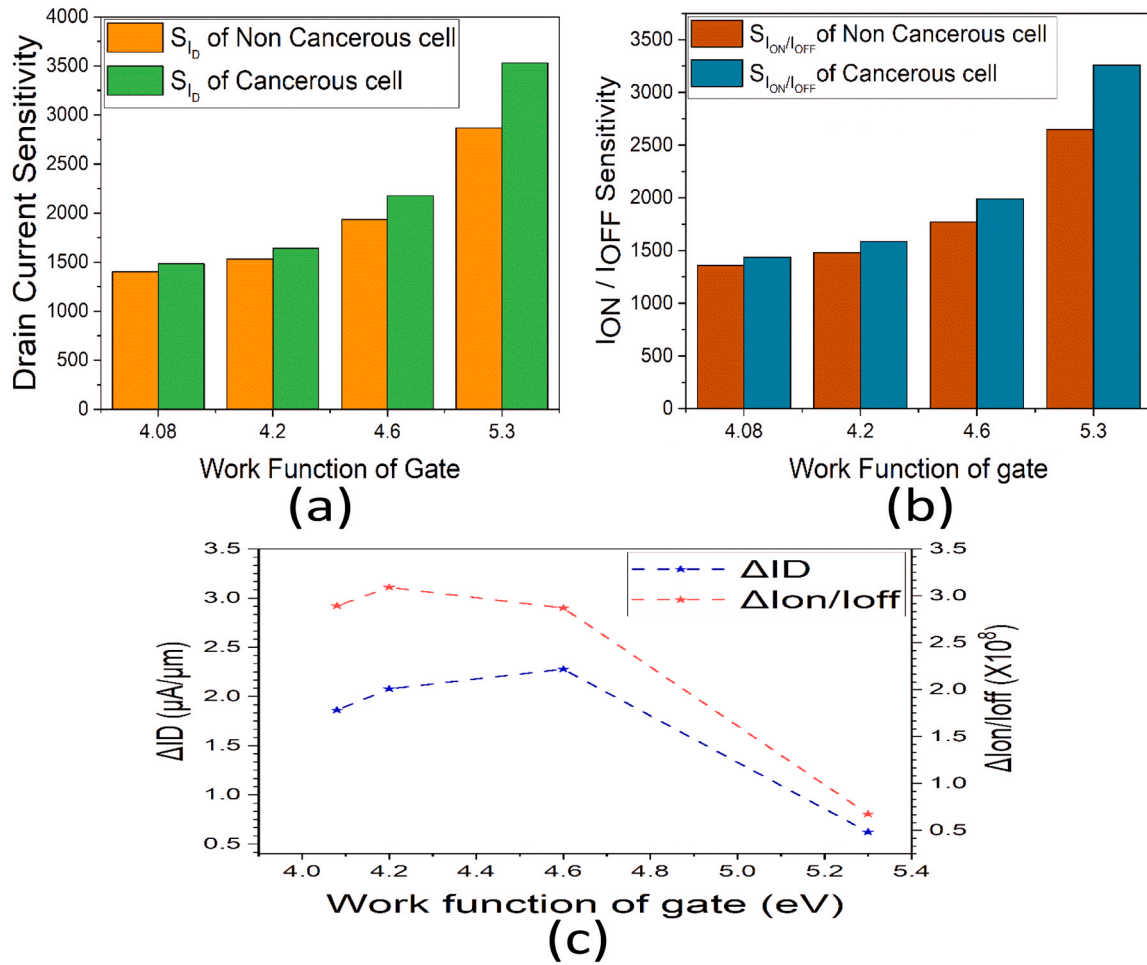


Fig. 9. (a) Drain current sensitivity, (b) I_{ON}/I_{OFF} sensitivity and (c) Differences in drain current and I_{ON}/I_{OFF} of silicon channel SEDGTFET device with different gate work function.

Table 1
 S_{ID} , $S_{I_{ON}/I_{OFF}}$, ΔI_D and $\Delta(I_{ON} / I_{OFF})$ for SEDGTFET devices having different channel material.

Channel Material	Cavity filling	S_{ID}	$S_{I_{ON}/I_{OFF}}$	ΔI_D ($\mu A / \mu m$)	$\Delta(I_{ON} / I_{OFF})$
Si	C	1641.817	1585.819	2.078	309154164
	NC	1533.397	1481.413		
Ge	C	1.290	2.3590	0.010	863.0601118
	NC	1.190	2.191		
GaAs	C	128.416	123.267	114.588	2.2178×10^{13}
	NC	114.330	110.819		

has been used along with the Auger model to ensure the recombination of carriers [39,40].

The data obtained has been contrasted with experimental data [41] given in Fig. 4 to compare the model with experimental. To have a close proximity between the modeled and experimental device, tunnelling masses has been considered as $0.039 \times$ rest tunnelling mass in BTBT model and the mole fraction of Ge in the SiGe layer is chosen as 0.45.

A further study is made on both SG and DG device at a frequency of 900 MHz in accordance with the cancerous and healthy liver cell lines implanted in the nano-cavities. At high frequencies, the healthy liver and cancerous liver cell line show different dielectric properties. The dielectric constants for healthy and cancerous liver samples are 51.10 and 57 respectively at 900 MHz [34]. For the identification of whether the specimen is cancerous or healthy, the transfer characteristics are plotted and the sensitivities have been calculated which has been

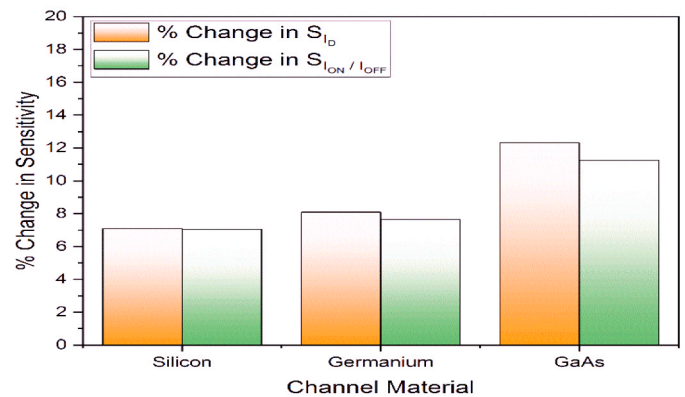


Fig. 10. Percentage change in drain current sensitivity and I_{ON}/I_{OFF} sensitivity of SEDGTFET device.

portrayed in the next section.

3. Results and discussion

Considering the cavities are filled with biomolecules for SEDGTFET and SEDGTFET structure, a relative study has been carried out, which is shown in this section. The drain current sensitivity (S_{ID}) and I_{ON}/I_{OFF} sensitivity ($S_{I_{ON}/I_{OFF}}$) has been taken for the qualitative assessment. For

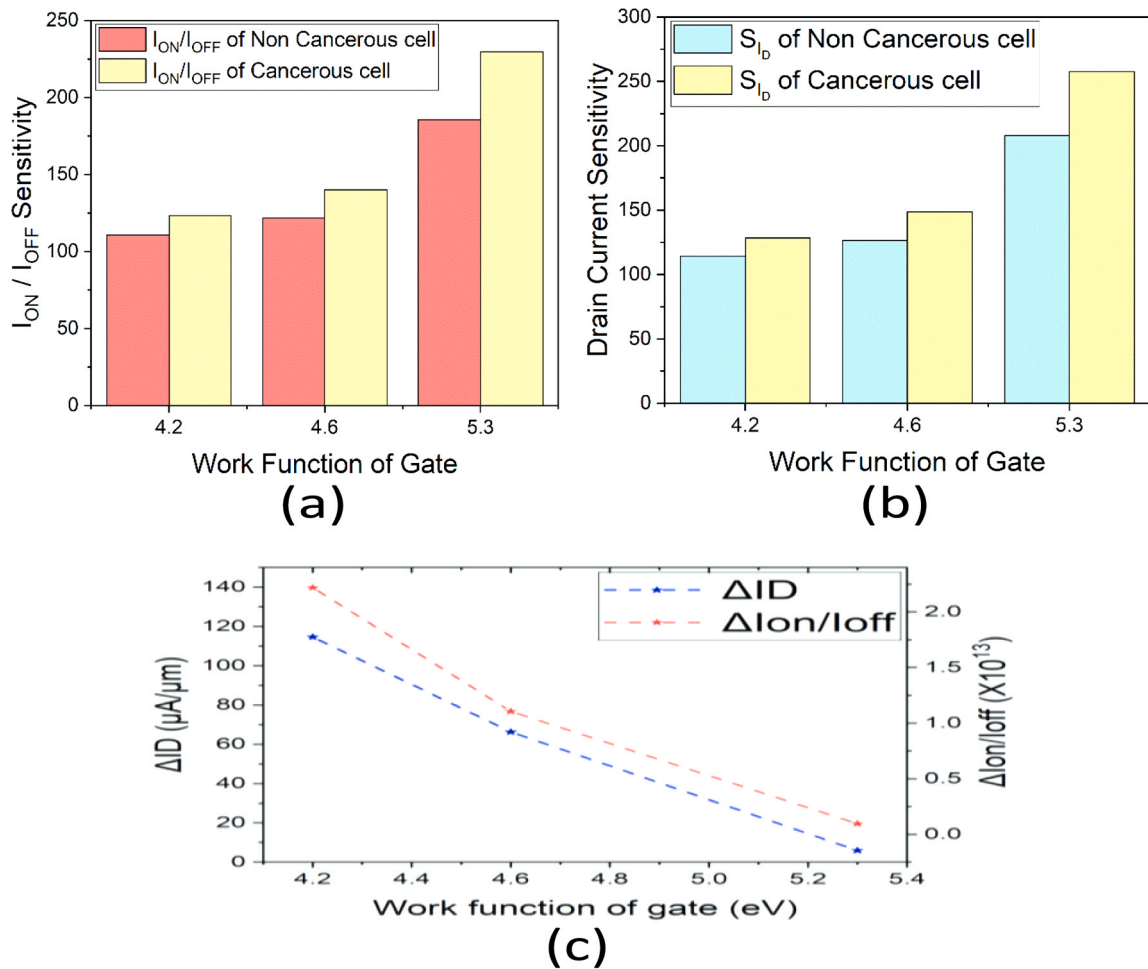


Fig. 11. (a) Drain current sensitivity, (b) I_{ON}/I_{OFF} sensitivity, (c) Differences in drain current and I_{ON}/I_{OFF} of GaAs channel SEDGTFET device with different gate work-functions.

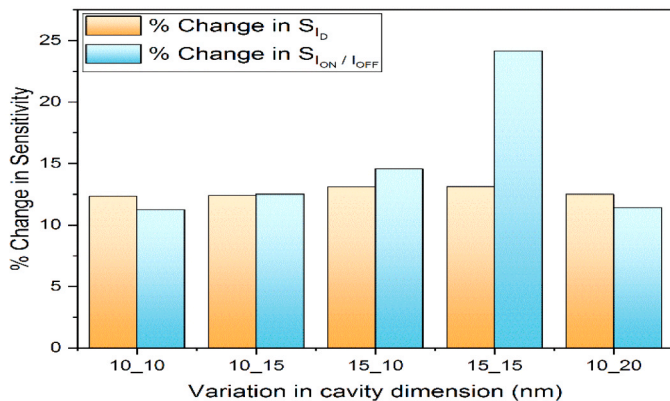


Fig. 12. Percentage change in S_{I_D} and $S_{I_{ON}/I_{OFF}}$ of GaAs channel SEDGTFET device with different cavity dimensions.

Table 2

ΔI_D and $\Delta(I_{ON} / I_{OFF})$ for GaAs channel devices having different cavity dimensions.

Cavity dimension	ΔI_D ($\mu A/\mu m$)	$\Delta (I_{ON} / I_{OFF})$
SC-10 nm, DC-10 nm	115	2.22×10^{13}
SC-10 nm, DC-15 nm	119	2.61×10^{13}
SC-15 nm, DC-10 nm	112	2.73×10^{13}
SC-15 nm, DC-15 nm	115	4.40×10^{13}
SC-10 nm, DC-20 nm	127	2.49×10^{13}

sensitivity calculation following equations have been considered.

$$S_{I_D} = \frac{I_{D (K>1)} - I_{D (K=1)}}{I_{D (K=1)}} \quad (1)$$

$$S_{I_{ON}/I_{OFF}} = \frac{I_{ON} / I_{OFF (K>1)} - I_{ON} / I_{OFF (K=1)}}{I_{ON} / I_{OFF (K=1)}} \quad (2)$$

Where $I_{D (K>1)}$ and $I_{ON} / I_{OFF (K>1)}$ has been considered as the drain current and ratio of ON and OFF current when the cavities are filled with the specimen; on the other hand $I_{D (K=1)}$ and $I_{ON} / I_{OFF (K=1)}$ refers to the same when the cavities are empty.

3.1. Performance of SESGTFET for various adhesive layers in the cavity

In Fig. 5, drain current has been shown in linear scale to indicate the

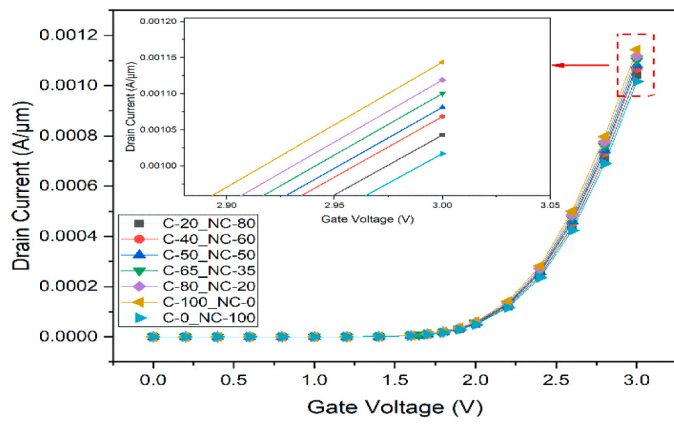


Fig. 13. Transfer Characteristics of GaAs channel SEDGTFET device with different percentages of C and NC liver cells.

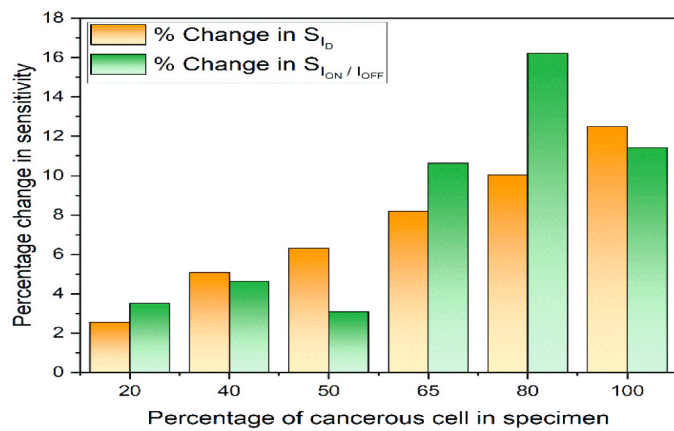


Fig. 14. Percentage change in S_{I_D} and $S_{I_{ON}/I_{OFF}}$ of GaAs channel SEDGTFET device with different percentage of C and NC liver cells.

Table 3
 S_{I_D} , $S_{I_{ON}/I_{OFF}}$ for GaAs channel SEDGTFET having different percentages of C and NC liver cells.

% of cancerous cell	S_{I_D}	% Change in S_{I_D}	$S_{I_{ON}/I_{OFF}}$	% Change in $S_{I_{ON}/I_{OFF}}$
20	493.9844	2.5450	487.9919	3.5180
40	506.1516	5.0708	493.1625	4.6148
50	512.1925	6.3248	485.9236	3.0792
65	521.2089	8.1965	521.5445	10.6355
80	530.1166	10.0456	547.8338	16.2123
100	541.8803	12.4876	525.1988	11.4107

change in drain current due to the presence of cancerous liver cell lines with respect to the healthy liver cell line in the cavities. SiO_2 , Silicon and HfO_2 has been taken into consideration as an adhesive layer in the cavity and it has been noticed that the S_{I_D} and $S_{I_{ON}/I_{OFF}}$ is better for SiO_2 . SiO_2 offers more band gap narrowing in the channel region, which results in shortening of the tunnelling path. As the tunneling path reduces the drain current in ON state increases and hence the sensitivities are much increased with respect to others in the SEDGTFET device. For SiO_2 adhesive layer the surface potential increases with respect to the other combination which also affects the drain current to increase hence same for the sensitivities also. Fig. 6(a) and 6(b) depict the comparison of S_{I_D} and $S_{I_{ON}/I_{OFF}}$ for healthy and cancerous liver cell lines with different combinations of adhesive layers in the cavity. In this study, the mole fraction of Ge in the SiGe layer has been considered as a nominal value of

0.15.

3.2. Performance analysis of SEDGTFET for various gate material

Fig. 7 depicts the transfer characteristics of the SG and DG structure in which the change in drain current for cancerous and non-cancerous liver cell lines has been observed. Due to the insertion of another gate in the SG device, the change in drain current has increased by 5%. As the changes in drain current are more for cancerous and healthy liver tissue the SEDGTFET can be a good candidate for the detection of liver cancer. In this section, a study has been carried out by considering the different gate metals.

Fig. 8 portrayed the transfer characteristics for different metal work functions for inserting cancerous (C) and non-cancerous (NC) liver cells. Figs. 9(a) and 9(b) present the S_{I_D} and $S_{I_{ON}/I_{OFF}}$ for different gate work functions, it can be observed that both sensitivities are more for work function 5.3 eV. But as the purpose of the device is to differentiate the cancerous liver cell from healthy cells another analysis has been considered which is based on the change in drain current and change in on and off current ratio for C and NC liver cell lines.

Change in drain current (ΔI_D) and change in I_{ON}/I_{OFF} ($\Delta(I_{ON} - I_{OFF})$) has been evaluated as follows.

$$\Delta I_D = I_{D(C)} - I_{D(H)} \tag{3}$$

$$\Delta(I_{ON} - I_{OFF}) = I_{ON(I_{OFF(C)})} - I_{ON(I_{OFF(H)})} \tag{4}$$

Where, $I_{D(C)}$, $I_{ON(I_{OFF(C)})}$ and $I_{D(H)}$, $I_{ON(I_{OFF(H)})}$ represents the drain current, I_{ON}/I_{OFF} for cancerous liver cells and healthy liver cells respectively. Fig. 9(c) represents the ΔI_D and $\Delta(I_{ON} - I_{OFF})$ for different gate metals and the plot exhibits that the change in drain current is more for 4.6 eV but the change in I_{ON}/I_{OFF} is more for 4.2 eV.

3.3. Performance analysis of SEDGTFET for various channel material

In this section of the analysis, the channel material has been modulated to have a comparative study for DG structure. Three materials have been considered as channel materials those are silicon (Si), germanium (Ge), and gallium arsenide (GaAs). Table-I portrayed S_{I_D} and $S_{I_{ON}/I_{OFF}}$ for different channel materials and from the same table it can be noticed that the sensitivities are better for Si channel devices with respect to others. But as the perspective of the work is to differentiate between cancerous and healthy liver cells, it is better to concentrate on the change in characteristics for cancerous and healthy liver cells, which can be observed in Table 1. From Table 1 it can be noted that the ΔI_D and $\Delta(I_{ON} - I_{OFF})$ is better for GaAs channel DG devices. In Fig. 10, the percentage change in sensitivities is shown for different combinations in which similar results have been observed. Considering the outcomes for this section, GaAs can be used as channel

material to obtain more change in characteristics in the presence and absence of cancerous liver cells in the specimen.

3.4. Performance of GaAs channel SEDGTFET for various gate material

This section of the study focuses on the gatework function modification of the GaAs channel SEDGTFET device. Figs. 11(a) and 11(b) depict the sensitivities of the device for different metal work-function. From the same figures, it can be observed that both sensitivities are more for devices with a metal work function of 5.3 eV due to the low drain current for the same device with a cavity filled with air. Another analysis has been done which has been presented in Fig. 11(c) where it can be noted that ΔI_D and $\Delta(I_{ON} - I_{OFF})$ is better for.

GaAs channel DG device for gate work function of 4.2 eV. GaAs channel DG device having 4.2 eV as gate work function offers better electric field in the channel region which promotes the drain current due

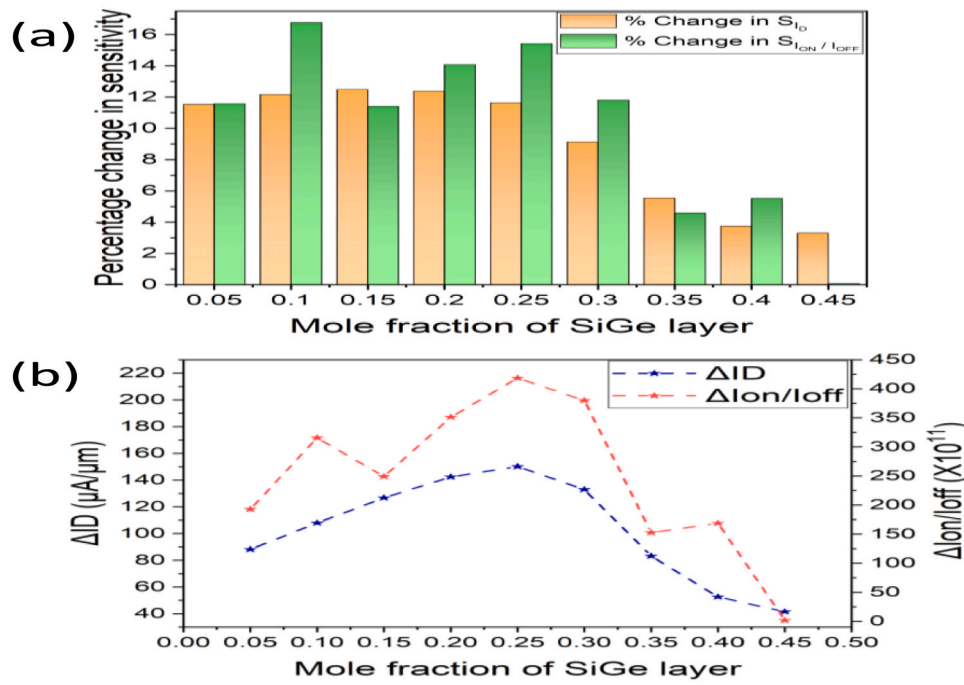


Fig. 15. (a) Percentage change in S_{I_D} and $S_{I_{ON}/I_{OFF}}$, (b) ΔI_D and $\Delta(I_{ON} / I_{OFF})$ of GaAs channel SEDGTFET device having different mole fraction of SiGe layer.

Table 4
Comparison between different methods for the detection of liver cancer.

Reference	Method	Target	Time
Aasi <i>et al.</i> [18] (Theoretical)	CNT	1-Octen-3-ol	~10 s
Wang <i>et al.</i> [43] (Experimental)	Cantilever based	AFP	Few hours
Chen <i>et al.</i> [44] (Experimental)	Aptamer-based microcantilever	HepG2	Few hours
Falahi <i>et al.</i> [45] (Theoretical)	Cantilever based	mRNA	Within 1 h
Liu <i>et al.</i> [46] (Experimental)	SERS	Blood serum	1 h
Owais <i>et al.</i> [47] (Experimental)	Chemical	Tumor cell surface-specific antibody	Few days
Wang <i>et al.</i> [48] (Theoretical)	Electrochemical	MXR7	Few hours
This work	FET	Liver cell	~10 s

Table 5
Comparison of the performance of the proposed device with the bio-sensor state-of-art.

Reference	Cavity Length & Width	FET based Bio-Sensor	S_{I_D}	$S_{I_{ON}/I_{OFF}}$
Wadhwa <i>et al.</i> [20]	8 & 2.5 nm	JLTFET	100	-
Goel <i>et al.</i> [22]	30 & 1 nm	JLNWFET	0.5	-
Singh <i>et al.</i> [49]	165 ⁰ & 0.8 nm	ArcTFET	-	210
Wangkheirakpam <i>et al.</i> [50]	15 & 5 nm	Vertical TFET	-	102
Verma <i>et al.</i> [51]	15 & 5 nm	Vertical TFET	150	120
This work	10 & 9 nm	SEDGTFET	541.88	525.19

to which ΔI_D and $\Delta(I_{ON} - I_{OFF})$ is better with respect to other combinations.

3.5. Performance of GaAs channel SEDGTFET for various cavity dimension

Considering the results obtained from the previous section an

investigation has been done by modulating the cavity length of the DG device for a metal gate work function of 4.2 eV. Fig. 12 shows the variation in percentage change in sensitivities for different cavity formations where '10_10' represents the source and drain side cavity having a length of 10 nm each. In the above-mentioned analysis, it has been observed that the percentage change in both the sensitivities is better for the device having a 15 nm source and drain side cavity with respect to the other combinations as for 15 nm source and drain side cavity device offers lesser drain current for the empty cavity.

Table 2 represents ΔI_D and $\Delta(I_{ON} - I_{OFF})$ for different combinations where it can be noted that for 10 nm and 20 nm source and drain side cavity devices the ΔI_D is more and $\Delta(I_{ON} - I_{OFF})$ is better considering 15 nm and 15 nm source and drain side cavities.

3.6. Performance analysis of GaAs channel SEDGTFET device for specimens having various proportions of cancerous cell

From the previous analysis, the device with 10 nm and 20 nm source and drain side cavity offers more. ΔI_D in this section the DG device has been tested considering the specimen having different percentages of cancerous and healthy liver cell. By Bruggeman's formula [42] the effective dielectric constant has been calculated considering the different proportions of cancerous liver cell in the specimen. The following equations has been considered for the analysis.

$$H_B = (2 - 3C_H)\epsilon_C - (1 - 3C_H)\epsilon_H \quad (5)$$

$$\epsilon_{eff} = \frac{H_B + \sqrt{H_B^2 + 8\epsilon_C\epsilon_H}}{4} \quad (6)$$

Where C_H is the fractional volume of healthy liver cell in and ϵ_C, ϵ_H are the dielectric constants of the cancerous and healthy liver cell respectively.

Fig. 13 depicts the GaAs channel SEDGTFET transfer characteristics with 10 nm and 20 nm source and drain side cavities considering the different percentages of cancerous cells. From the above-mentioned analysis, it can be noted that the proposed device is able to detect the various percentage of liver cancer cells in the target specimen.

Fig. 14 presents the percentage change in sensitivity for different

specimens containing different percentages of cancerous liver cells. As the purpose is to differentiate the cancerous and healthy liver cells the above-mentioned analysis is important. The sensitivities for different cases have been tabulated in Table 3 to have a comparative study.

3.7. Performance analysis of GaAs channel SEDGTFET device for different mole fractions of SiGe layer

In this section, a comparative study has been conducted for GaAs channel SEDGTFET structure with 10 nm and 20 nm source and drain side cavity considering various mole fractions of the SiGe layer in the channel region. With the increase in mole fraction, the device drain current increases for empty cavities due to the increased surface potential of the device as a result it has been observed that both the sensitivities have been decreased by increasing the mole fraction of SiGe layer. Fig. 15(a) depicts the percentage change in sensitivities with respect to the different mole fractions of the SiGe layer in which it can be observed that the performance of the device is better with respect to the others for 0.15 mol fraction in terms of change in drain current sensitivity. But if the analysis has been done on the basis of percentage change in $S_{I_{ON}/I_{OFF}}$ then the device with 0.1 mol fraction gives a better result. Fig. 15(b) presents ΔI_D and $\Delta(I_{ON} - I_{OFF})$ for DG devices with different mole fractions, it can be seen that the above-mentioned parameters are better for the device with mole fraction 0.25 with respect to the other device with other mole fractions of SiGe layer. So, from this analysis, it can be noted that the device with a 0.25 mol fraction can be a good candidate for differentiating cancerous and non-cancerous liver cells.

4. Comparative analysis

A comparative investigation has been conducted to examine the performance of the proposed device. Table 4 includes a list of many methods for detecting liver cancer along with the suggested procedure, allowing for a comparison of the various methods reported in the literature. Table 5 compares the performances of the proposed device with other popular FET structures available in literature where a substantial change in sensitivities can be observed for the proposed device.

5. Conclusion

For the purpose of detecting liver cancer, a source extended single gate device with both side cavities has been employed in this work. SiO₂ has been found to offer greater sensitivity than bare silicon and HfO₂ as an adhesive layer in the cavity region. To differentiate the cancerous and non-cancerous liver cells, the change in drain current has been considered as an important parameter besides the sensitivity analysis. In this context, the SEDGTFET structure offers more change in drain current. The SEDGTFET with the gate work function of 5.3 eV results in more change in sensitivities, although the change in drain current and ON-OFF ratio is more if the work function is 4.6 eV. By altering the channel material, it has been perceived that the percentage change in sensitivities and change in drain current and ON-OFF ratio are greater by considering GaAs as channel material, which can reduce the cost of the measuring device. The GaAs channel SEDGTFET with 5.3 eV as gate work function improves sensitivities, but considering the purpose of differentiating cancerous and non-cancerous liver cells, the change in drain current and ON-OFF ratio has been studied. The above-mentioned parameters are more by considering the gate work function of 4.2 eV in GaAs channel SEDGTFET device. In the above-mentioned device, the change in drain current is maximum if the structure has a source and drain side cavity of 10 nm and 20 nm, respectively and the change in the ON-OFF ratio of drain current is more if the source and drain side cavity of 15 nm each. The proposed GaAs channel SEDGTFET device can also detect the cancerous liver cell present in the specimen in smaller percentages. Another analysis has been conducted by varying the mole

fraction of SiGe layer in the device, and it has been noted that for 0.25 mol fraction, the change in drain current and ON-OFF ratio of drain current is more. The comparison of the proposed device with the existing device shows a significant change in sensitivity parameters. From the study, it can be concluded that the proposed method promotes POC diagnosis as this method effectively detect the cancerous liver cell from the target specimen.

CRedit authorship contribution statement

Kumar Amitesh: Writing – review & editing, Supervision, Software, Resources, Project administration, Funding acquisition. **Kolay Anirban:** Writing – original draft, Methodology, Formal analysis, Data curation, Conceptualization.

Declaration of Competing Interest

The authors declare that they have no known competing financial interests or personal relationships that could have appeared to influence the work reported in this paper.

Data availability

The authors are unable or have chosen not to specify which data has been used.

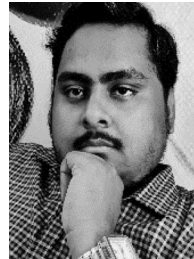
Acknowledgment

The authors acknowledge the Department of Science and Technology (DST), Govt. of India for the financial assistance provided under DST SERB Project (File No. SRG/2021/002110) to carry out the present work. Authors would like to thank NIT Patna for providing research facilities.

References

- [1] D. Mzurikwao, M.U. Khan, O.W. Samuel, J. Cinatl Jr, M. Wass, M. Michaelis, et al., Towards image-based cancer cell lines authentication using deep neural networks, *Sci. Rep.* 10 (2020).
- [2] B.E. da Silva, L.M. de Lemos, A.R. Moura, Y.A. Ferrari, M.S. Lima, Oliveira de, M. Santos, C.A. Lima, Gynaecological cancer incidence and mortality trends in a Brazilian State with medium human development index: a 22-year analysis, *Cancer Epidemiol.* 88 (2024 1) 102493.
- [3] H. Al Maliki, K.J. Monahan, The diagnostic yield of colonoscopic surveillance following resection of early age onset colorectal cancer, *U. Eur. Gastroenterol. J.* (2024 3).
- [4] J. Ferlay, M. Ervik, F. Lam, M. Colombet, L. Mery, M. Piñeros, et al., Global Cancer Observatory: Cancer Today, International Agency for Research on Cancer, Lyon, 2020 (<https://gco.iarc.fr/today>, accessed October 2022).
- [5] E. Vorontsov, M. Cerny, P. R gnier, L. Di Jorio, C.J. Pal, R. Lapointe, et al., Deep learning for automated segmentation of liver lesions at CT in patients with colorectal cancer liver metastases, *Radiol. Artif. Intell.* 1 (2019) 180014.
- [6] C. Mezzacappa, R. Rossi, A. Jaffe, T.H. Taddei, M. Strazzabosco, Community-level factors associated with hepatocellular carcinoma incidence and mortality: an observational registry study, *Cancer Epidemiol., Biomark. Prev.* (2024). Jan 3:OF1-9.
- [7] M.C.S. Wong, J.Y. Jiang, W.B. Goggins, M. Liang, Y. Fang, F.D.H. Fung, et al., International incidence and mortality trends of liver cancer: a global profile, *Sci. Rep.* 7 (2017).
- [8] S.-N. Lu, J.-H. Wang, K.-M. Kee, P.-L. Tseng, Screening with ultrasonography of patients at high-risk for hepatocellular carcinoma: thrombocytopenia as a valid surrogate of cirrhosis, *Liver Cancer* (2009) 137–144.
- [9] S.H. Lin, K.T. Wu, C.C. Wang, K.T. Huang, L.W. Hsu, H.L. Eng, K.W. Chiu, Immune responses to anti-hepatitis C virus antibodies during pre-liver transplantation direct-acting antiviral therapy in hepatitis C virus-infected recipients associated with post-liver transplantation allograft injury, *Antibodies* 13 (1) (2024) 7.
- [10] H.B. El-Serag, J.A. Marrero, L. Rudolph, K.R. Reddy, Diagnosis and Treatment of Hepatocellular Carcinoma, *Gastroenterology* 134 (2008) 1752–1763.
- [11] J.F. Cadranel, C. Buffet, P. Cauquil, O. Ink, D. Pariente, J.P. Etienne, Nodules pseudo-tumoraux du foie chez le cirrhotique. Etude de 7 cas, *GastroenteArol Clin. Biol.* 12 (1988) 833–840.
- [12] W.J. Miller, R.L. Baron, G.D. Dodd 3rd, M.P. Federle, Malignancies in patients with cirrhosis: CT sensitivity and specificity in 200 consecutive transplant patients, *Radiology* 193 (1994) 645–650.

- [13] U.S. Dinish, G. Balasundaram, Y.-T. Chang, M. Olivo, Actively targeted in vivo multiplex detection of intrinsic cancer biomarkers using biocompatible SERS nanotags, *Sci. Rep.* 4 (2014).
- [14] A. Futane, V. Narayanamurthy, P. Jadhav, A. Srinivasan, Aptamer-based rapid diagnosis for point-of-care application, *Microfluid Nanofluid* 27 (2023).
- [15] Z.-F. Sun, Y. Chang, N. Xia, Recent development of nanomaterials-based cytosensors for the detection of circulating tumor cells, *Biosensors* 11 (2021) 281.
- [16] D. Sun, J. Lu, Z. Chen, Y. Yu, M. Mo, A repeatable assembling and disassembling electrochemical aptamer cytosensor for ultrasensitive and highly selective detection of human liver cancer cells, *Anal. Chim. Acta* 885 (2015) 166–173.
- [17] E. Ahmadian, D. Janas, A. Eftekhari, N. Zare, Application of carbon nanotubes in sensing/monitoring of pancreas and liver cancer, *Chemosphere* 302 (2022) 134826.
- [18] A. Aasi, E. Aasi, S. Mehdi Aghaei, B. Panchapakesan, CNT biodevices for early liver cancer diagnosis based on biomarkers detection- a promising platform, *J. Mol. Graph. Model.* 114 (2022) 108208.
- [19] P. Bergveld, Development of an ion-sensitive solid-state device for neurophysiological measurements, *IEEE Trans. Biomed. Eng.* (1970). BME-17: 70–1.
- [20] G. Wadhwa, B. Raj, Design, simulation and performance analysis of JLTFT biosensor for high sensitivity, *IEEE Trans. Nanotechnol.* 18 (2019) 567–574.
- [21] S. Ebrahimi, Z. Ebrahim Nataj, S. Khodaverdian, A. Khamsavi, Y. Abdi, K. Khajeh, An ion-sensitive field-effect transistor biosensor based on SWCNT and aligned MWCNTs for detection of ABTS, *IEEE Sens. J.* 20 (2020) 14590–14597.
- [22] A. Goel, S. Rewari, S. Verma, S.S. Deswal, R.S. Gupta, Dielectric modulated junctionless biotube FET (DM-JL-BT-FET) bio-sensor, *IEEE Sens. J.* 21 (2021) 16731–16743.
- [23] S. Tayal, B. Majumdar, S. Bhattacharya, S. Kanungo, Performance analysis of the dielectrically modulated junction-less nanotube field effect transistor for biomolecule detection, *IEEE Trans. Nanobioscience* 22 (2023) 174–181.
- [24] J. Bitra, G. Komanapalli, A comprehensive performance investigation on junction-less TFET (JL-TFET) based biosensor: device structure and sensitivity, *Trans. Electr. Electron Mater.* 24 (2023) 365–372.
- [25] C. Chong, H. Liu, S. Wang, S. Chen, Simulation and performance analysis of dielectric modulated dual source trench gate TFET biosensor, *Nanoscale Res Lett.* 16 (2021).
- [26] P. Vimala, L.L. Krishna, S.S. Sharma, TFET biosensor simulation and analysis for various biomolecules, *Silicon* 14 (2022) 7933–7938.
- [27] R. Abdunnassir, A. Singh, D. Tekilu, G. Subarao, M. Chanda, Assessment of hetero-structure junction-less tunnel FET's efficacy for biosensing applications, *Sens Imaging* 25 (2023).
- [28] Y. Yang, B. Zeng, Y. Li, H. Liang, Y. Yang, Q. Yuan, Construction of MoS₂ field effect transistor sensor array for the detection of bladder cancer biomarkers, *Sci. China Chem.* 63 (2020) 997–1003.
- [29] Y. Zhang, D. Feng, Y. Xu, Z. Yin, W. Dou, U.E. Habiba, et al., DNA-based functionalisation of two-dimensional MoS₂ FET biosensor for ultrasensitive detection of PSA, *Appl. Surf. Sci.* 548 (2021) 149169.
- [30] Rajesh, Z. Gao, R. Vishnubhotla, P. Ducos, M.D. Serrano, J. Ping, et al., Genetically engineered antibody functionalized platinum nanoparticles modified CVD-graphene nanohybrid transistor for the detection of breast cancer biomarker, HER3, *Adv. Mater. Inter* 3 (2016).
- [31] C.-C. Huang, Y.-H. Kuo, Y.-S. Chen, P.-C. Huang, G.-B. Lee, A miniaturised, DNA-FET biosensor-based microfluidic system for quantification of two breast cancer biomarkers, *Microfluid Nanofluid* 25 (2021).
- [32] G. Yang, Z. Xiao, C. Tang, Y. Deng, H. Huang, Z. He, Recent advances in biosensor for detection of lung cancer biomarkers, *Biosens. Bioelectron.* 141 (2019) 111416.
- [33] A. Peyman, B. Kos, M. Djokić, B. Trovovšek, C. Limbaeck-Stokin, G. Serša, et al., Variation in dielectric properties due to pathological changes in human liver, *Bioelectromagnetics* 36 (2015) 603–612.
- [34] W.T. Joines, Y. Zhang, C. Li, R.L. Jirtle, The measured electrical properties of normal and malignant human tissues from 50 to 900 MHz, *Med. Phys.* 21 (1994) 547–550.
- [35] S. Nuciforo, I. Fofana, M.S. Matter, T. Blumer, D. Calabrese, T. Boldanova, et al., Organoid models of human liver cancers derived from tumor needle biopsies, *Cell Rep.* 24 (2018) 1363–1376.
- [36] ATLAS Device Simulation Software and manual. Santa Clara, CA, USA: Silvaco Int. 2018.
- [37] S. Chen, S. Wang, H. Liu, T. Han, H. Xie, C. Chong, A novel dopingless fin-shaped SiGe channel TFET with improved performance, *Nanoscale Res Lett.* 15 (2020).
- [38] S. Singh, B. Raj, Modeling and simulation analysis of SiGe heterojunction Double Gate Vertical t-shaped tunnel FET, *Superlattices Microstruct.* 142 (2020) 106496.
- [39] M. Zhang, Y. Guo, J. Zhang, J. Yao, J. Chen, Simulation study of the double-gate tunnel field-effect transistor with step channel thickness, *Nanoscale Res Lett.* 15 (2020).
- [40] S.-C. Teng, Y.-S. Su, Y.-H. Wu, Design and simulation of improved swing and ambipolar effect for tunnel FET by band engineering using metal silicide at drain side, *IEEE Trans. Nanotechnol.* 18 (2019) 274–278.
- [41] A.M. Walke, A. Vandooren, R. Rooyackers, D. Leonelli, A. Hikavvy, R. Loo, et al., Fabrication and Analysis of a Si/Si_{0.55}Ge_{0.45} Heterojunction Line Tunnel FET, *IEEE Trans. Electron Devices* 61 (2014) 707–715.
- [42] J. Sukham, O. Takayama, M. Mahmoodi, S. Sychev, A. Bogdanov, S.H. Tavassoli, A. V. Lavrinenko, R. Malureanu, Investigation of effective media applicability for ultrathin multilayer structures, *Nanoscale* 11 (26) (2019) 12582–12588.
- [43] S. Wang, J. Wang, Y. Zhu, J. Yang, F. Yang, A new device for liver cancer biomarker detection with high accuracy, *Sens. Bio-Sens. Res.* 4 (2015) 40–45.
- [44] X. Chen, Y. Pan, H. Liu, X. Bai, N. Wang, B. Zhang, Label-free detection of liver cancer cells by aptamer-based microcantilever biosensor, *Biosens. Bioelectron.* 79 (2016) 353–358.
- [45] S. Falahi, H.-A. Rafiee-Pour, M. Zarejousheghani, P. Rahimi, Y. Joseph, Non-coding RNA-based biosensors for early detection of liver cancer, *Biomedicines* 9 (2021) 964.
- [46] R. Liu, Y. Xiong, Y. Guo, M. Si, W. Tang, Label-free and non-invasive BS-SERS detection of liver cancer based on the solid device of silver nanofilm, *J. Raman Spectrosc.* 49 (2018) 1426–1434.
- [47] Owais, M. Chauhan, A. Tufail, Sherwani, M. Sajid, C.R. Suri, et al., Fungus-mediated biological synthesis of gold nanoparticles: potential in detection of liver cancer, *IJN* (2011) 2305.
- [48] M. Wang, Y. Tang, Y. Chen, Y. Cao, G. Chen, Catalytic hairpin assembly-programmed formation of clickable nucleic acids for electrochemical detection of liver cancer related short gene, *Anal. Chim. Acta* 1045 (2019) 77–84.
- [49] N.K. Singh, R. Kar, D. Mandal, Simulation study of novel charge-plasma based ArcTFET for sensing the breast cancer biomarker (C-erbB-2) in serum, *IEEE Trans. Nanobioscience* 22 (2023) 554–561.
- [50] V.D. Wangkheirakpam, B. Bhowmick, P.D. Pukhrabam, N+ pocket doped vertical TFET based dielectric-modulated biosensor considering non-ideal hybridization issue: a simulation study, *IEEE Trans. Nanotechnol.* 19 (2020) 156–162.
- [51] M. Verma, S. Tirkey, S. Yadav, D. Sharma, D.S. Yadav, Performance assessment of a novel vertical dielectrically modulated TFET-based biosensor, *IEEE Trans. Electron Devices* 64 (2017) 3841–3848.



Anirban Kolay received the M.Tech degree in Electrical Engineering from Calcutta University, West Bengal, India, in 2014 and B.Tech degree in Electrical Engineering from Burdwan University, Burdwan, India, in 2012. He currently works as an assistant professor at the Department of Electrical Engineering, Heritage Institute of Technology, Kolkata. His current research interests include the semiconductor devices modeling and development of semiconductor devices-based biosensors for detection of various biomolecules.



Amitesh Kumar has done his B.Tech in Electrical Engineering from Indian Institute of Technology, BHU. He did his Ph.D. in Electrical Engineering from Indian Institute of Technology, Indore. He did his Postdoc Research from University of Utah, USA. He has been a Research Fellow awardee from CSIR, Govt. of India. He is currently working as Assistant Professor in Electrical Engineering at National Institute of Technology, Patna.